

Ultrafast Study of Charge Generation in Silole:Fluorene Mixed Film for Color Selective Organic Photoconductive Device

Takeshi Fukuda^{*1}, Ryohei Kobayashi¹, Zentaro Honda¹, Norihiko Kamata¹, Keita Mori¹, Yuu Suzuki¹, Ken Hatano¹, Akihiro Furube²

¹ Department of Functional Materials Science, Saitama University, 255 Shimo-Okubo, Sakura-ku, Saitama-shi, Saitama, 338-8570 Japan

² National Institute of Advanced Industrial Science and Technology, Central 5, 1-1-1 Higashi, Tsukuba, Ibaraki 305-8565, Japan

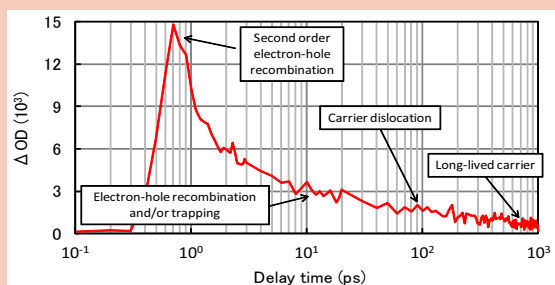
Received XXXX, revised XXXX, accepted XXXX

Published online XXXX

PACS 73.50.Pz, 82.53.Eb, 72.20.Jv, 78.20.-e, 33.80.Gj

* Corresponding author: e-mail fukuda@fms.saitama-u.ac.jp, Phone: +81-48-858-3526, Fax: +81-48-858-3526

Transient absorption characteristics of blue-sensitive organic thin films were investigated via a femtosecond pump-probe technique to estimate carrier kinetics. The most important finding is that the long-lived absorbance at 3440 nm increased with increasing the concentration of 1,1-dimethyl-2,5-bis(*N,N*-dimethylaminophenyl)-3,4-diphenylsilole (NMe₂-silole). This fact indicates photo-excited carriers were dislocated in the organic layer, and the doping of NMe₂-silole is considered to be useful method to improve photoconductive characteristics of organic devices.



Carrier kinetics model for NMe₂-silole doped F8BT.

Copyright line will be provided by the publisher

1 Introduction Organic materials have special optical and electrical properties for light-emitting diodes, photoconductive devices, and thin film transistors. By now, several research groups reported novel organic devices fabricated by solution processes, such as photovoltaic cells [1, 2] and sensors [3]. In addition, color selective organic photoconductive devices have been attracting considerable attention for stacked organic image sensor instead of Si-based charge coupled devices and complementary metal oxide semiconductor sensors [4–6]. This is because absorption coefficients of several organic materials are higher than that of Si at a visible wavelength region. This fact indicates most of the incident light is absorbed into the photoconductive layer, resulting in the high resolution sensing.

A previous paper demonstrated superior color selectivity of solution-processed organic photoconductive devices

at blue, green, and red regions [6]. A low carrier recombination probability in an organic layer is important factor for the efficient photo-excited carrier transport to electrodes. However, it is difficult to realize in the case of single layer structures. This fact causes lower external quantum efficiencies (EQEs) of solution-processed devices than those of multilayer structures fabricated by conventional thermal evaporation method [7].

By now, our research group reported an improved photoconductive characteristics of blue-sensitive organic devices by doping silole derivatives into poly(dioctylfluorenyl-co-benzo-thiadiazole) (F8BT) [8, 9]. Several silole derivatives acted as an electron acceptor into F8BT. Therefore, photo-induced electrons efficiently moved to the silole side, resulting in the formation of carrier dislocation. In addition, several silole derivatives showed superior electri-

Copyright line will be provided by the publisher

cal characteristics for organic devices, and they were used for an electron transport layer of organic light-emitting diodes owing to its high electron mobility [10, 11].

Transient absorption characteristics at the infrared (IR) region are useful tool to understand carrier kinetics after the irradiation of excited light [12, 13]. In this study, we investigated carrier kinetics in the NMe₂-silole doped F8BT film by measuring transient absorption characteristics at an infrared wavelength (3440 nm).

2 Experimental After dissolving F8BT into chloroform at a concentration of 1 wt%, NMe₂-silole was added into in a same vessel. The ratio of NMe₂-silole:F8BT (NMe₂-silole/(NMe₂-silole+F8BT)) was changed as 0, 12, 34, 45 and 62 wt% to investigate the relationship between the concentration of NMe₂-silole and the amount of photo-excited carriers into NMe₂-silole doped F8BT. A NMe₂-silole doped F8BT layer was spin-coated on a cleaned silica glass substrate. Then, the sample was annealed at 70 °C for 30 minutes to remove chloroform. Finally, an encapsulating glass substrate was covered to prevent the degradation of the organic layer.

We used ultrafast IR-probe femtosecond transient absorption spectroscopy to measure charge carrier kinetics. IR light is sensitive to charged carriers, namely electrons and holes, and delocalized excitons. In a later time scale near 1 ns, it is expected to observe charged species of holes in NMe₂-silole and electrons in F8BT judging from our previous work on the device performance [9]. Some details of the measurement system have been described previously[14]. The wavelength of pump light was 480 nm and that of probe light was 3440 nm. The excitation repetition was 500 Hz, and the temporal resolution was about 250 fs. The pump beam radius on the film surface was about 0.3 mm. All the transient absorption measurements were performed at 295 K. In addition, the absorption spectrum of the NMe₂-silole doped F8BT film was recorded with a double-beam UV-Vis spectrophotometer (JASCO, V-650).

3 Results and Discussion Figure 1 shows UV-Vis absorption spectra of NMe₂-silole doped F8BT films. The peak absorption coefficient decreased with the increasing concentration of NMe₂-silole. The minimum peak absorption coefficient was $8 \times 10^4 \text{ cm}^{-1}$ in the case of 62 wt% doped film. However, this value was high enough to absorb the pump light with the center wavelength of 480 nm.

Observed transient absorption kinetics for the NMe₂-silole (62 wt%) doped F8BT film is shown as a dependence of the excitation power from 0.05 to 0.4 mW in Fig. 2. The signal rise at the excitation timing is due to exciton generation and/or charge generation of electrons in NMe₂-silole and holes in F8BT. Although separation of these species is difficult at present, it is sure that species remaining up to the nanosecond time scale is due to charged species. Therefore we can evaluate relative charge generation efficiency from signal sizes at the later time region. Details of the

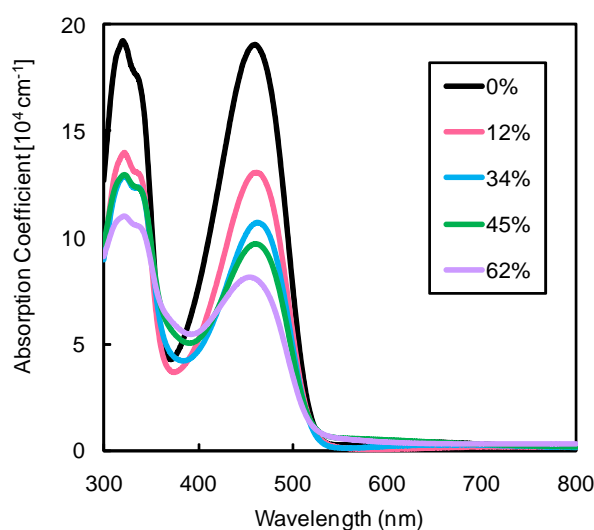


Figure 1 Absorption spectrum of NMe₂-silole doped F8BT film.

kinetics in the earlier time region are now under investigation and will be published elsewhere. Roughly speaking, however, sub-picosecond decay that became faster for the higher pump intensity can be assigned to second order recombination of excitons and/or charged species, and decay in 10-to-100 ps time scale, the rate of which was independent on the pump intensity, seems to be due to trapping and/or first order recombination process of them.

Figure 3(a) shows transient absorption kinetics for the NMe₂-silole doped F8BT films with different doping con-

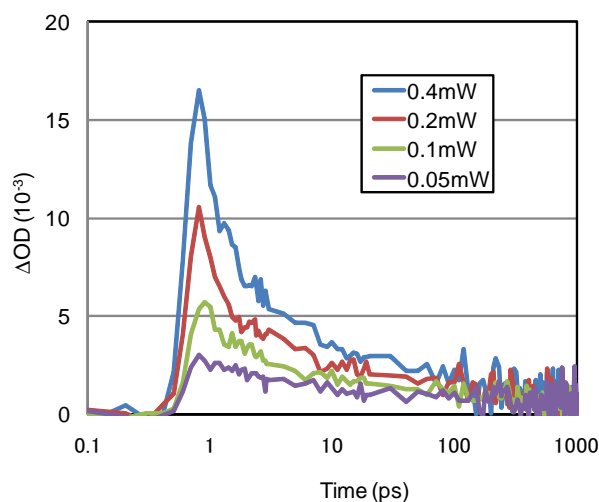
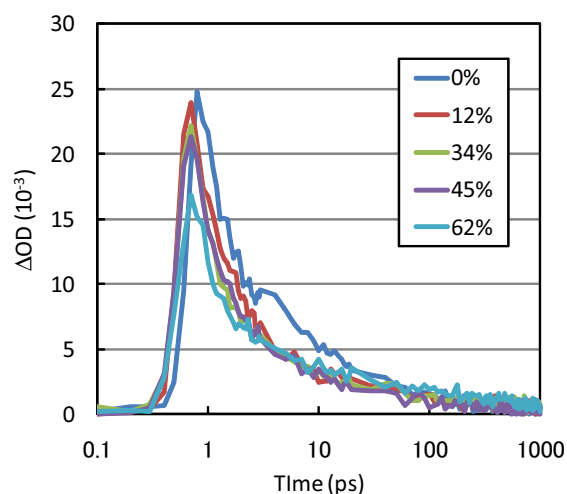


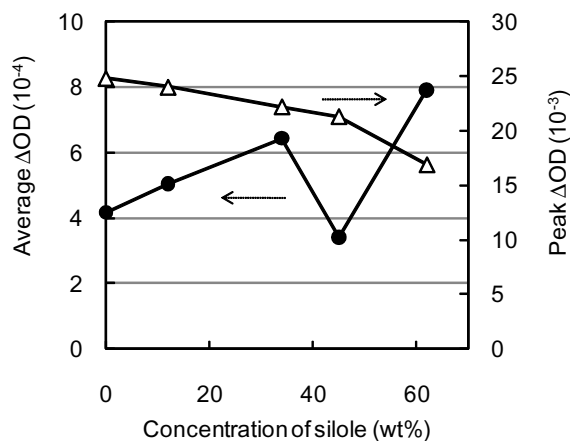
Figure 2 Transient decay kinetics for a NMe₂-silole (62 wt%) doped F8BT film following excitation at 480 nm. Decay kinetics were probed at 3440 nm. Excitation intensity was ranged from 0.05 mW to 0.4 mW.

centrations from 0 to 62 wt%. The optical intensity of pump light was 0.2 mW. The transient absorption signal sizes were corrected using absorption fraction at 480 nm in order to cancel the effect of different numbers of absorbed photons. It is seen that transient absorption just after excitation decreased with increasing NMe₂-silole concentration (shown in Fig. 3(b)). This tendency suggests that charge separation between NMe₂-silole and F8BT occurs within the time resolution (~ 250 fs). To obtain more direct evidences of charge separation process visible-region transient absorption experiments will be examined. Transient absorption intensities averaged between 500 ps and 1 ns are plotted against the concentrations of NMe₂-silole in Fig.

3(b). The increasing absorption for the larger silole concentration (except for the 45 wt% sample) indicates that charge carrier generation efficiency increased due to higher possibility of charge transfer at silole/F8BT interface. Well-dispersed silole starts to form aggregates at higher doping levels, making segregated silole structures beside F8BT regions. A microscope image of fabricated sample showed the most aggregated silole derivative at the concentration of 45 wt%. Therefore, this may be the reason of the charge generation efficiency drop at the 45 wt% doping. The increase of the efficiency at the 62 wt% doping case may be due to appearance of well-dispersed silole within F8BT region in addition to the segregated aggregates.



(a)



(b)

Figure 3 (a) Transient decay kinetics probed at 3440 nm for NMe₂-silole doped F8BT film following excitation at 480 nm. Concentration of NMe₂-silole doped F8BT film was ranged from 0 to 62 wt%. (b) Peak ΔOD and average ΔOD from 500 to 1000 ps as a function of the concentration of NMe₂-silole doped F8BT.

4 Conclusion We estimated the carrier kinetics for a NMe₂-silole doped F8BT by using femtosecond pump-probe technique. The long-lived average ΔOD from 500 to 1000 ps increased with increasing the concentration of NMe₂-silole. This result indicates photo-excited carriers efficiently dislocated in the F8BT layer by doping NMe₂-silole.

Acknowledgements The part of this work was supported by CASIO foundation.

References

- [1] L. Smilowitz, N.S. Sariciftci, R. Wu, C. Gettinger, A.J. Heeger, and F. Wudl, *Phys. Rev. B* **47**, 13835 (1993)
- [2] S. Günes, H. Neugebauer, and N.S. Sariciftci, *Chem. Rev.* **107**, 1324 (2007).
- [3] T. Someya, and T. Sekitani, *Procedia Chem.* **1**, 9 (2009).
- [4] B. Lamprecht, R. Thunauer, S. Kostler, G. Jakopic, G. Leising, and J. R. Krenn, *Phys. Stat. Sol. Rapid Res. Lett.* **2**, 178 (2008).
- [5] S. Aihara, H. Seo, M. Namba, T. Watabe, H. Ohtake, M. Kubota, N. Egami, T. Hiramatsu, T. Matsuda, M. Furuta, H. Nitta, and T. Hirao, *IEEE Trans. Electron.* **56**, 2570 (2009).
- [6] T. Fukuda, M. Komoriya, R. Kobayashi, Y. Ishimaru, and N. Kamata, *Jpn. J. Appl. Phys.* **48**, 04C162 (2009).
- [7] H. Seo, S. Aihara, T. Watabe, H. Ohtake, M. Kubota, and Norifumi Egami, *Jpn. J. Appl. Phys.* **46**, L1240 (2007).
- [8] T. Fukuda, R. Kobayashi, N. Kamata, S. Aihara, H. Seo, K. Hatano, and D. Terunuma, *Jpn. J. Appl. Phys.* **49**, 01AC05 (2010).
- [9] R. Kobayashi, T. Fukuda, Y. Suzuki, K. Hatano, N. Kamata, S. Aihara, H. Seo, and D. Terunuma, *Mol. Cry. Liq. Cry.* **519**, 206 (2010).
- [10] S. Yamaguchi, and K. Tamao, *J. Organomet. Chem.* **653**, 223 (2002).
- [11] H. Habrard, T. Ouisse, O. Stéphan, L. Aubouy, Ph. Gerbier, L. Hirsch, N. Huby, and A. Van der Lee, **156**, 1262 (2006).
- [12] E. Frankevich, J.G. Müller, and U. Lemmer, *Chem Phys.* **285**, 13 (2002).
- [13] S. Cook, R. Katoh, and A. Furube, *J. Phys. Chem. C* **113**, 2547 (2009).
- [14] L. Du, A. Furube, K. Hara, R. Katoh, and M. Tachiya, *Thin Solid Films* **518**, 861 (2009).